Control Strategies for a Hybrid Seven-level Inverter

Richard Lund+ Madhav D. Manjrekar# Peter Steimer* Thomas A. Lipo#

+Norges Teknisk-Naturvitenskapelige Universitet, Norway.

#Department of Electrical and Computer Engineering
University of Wisconsin – Madison
1415 Engineering Drive
Madison, WI 53706, USA.

*ABB Industrie AG, Dept. IA, 5300 Turgi, Switzerland.

Keywords

Control, Converter circuits, Drives, Emerging topologies, FACTS, Multilevel converters, New Devices.

Abstract

This paper is devoted to the investigation of control techniques applicable for seven-level 4.16 kV hybrid inverter. A detailed analysis of a hybrid modulation technique, which incorporates stepped synthesis in conjunction with variable pulse width of the consecutive steps, is included. In addition, variations of multicarrier Pulse Width Modulation (PWM) techniques related to the disposition and phase shifting and their comparative evaluation is presented in this paper. The performance attributes of conventional techniques such as staircase modulation and programmed PWM are assessed and optimization of switching angles to minimize the harmonic distortion at different modulation depths is discussed. Operating principles, spectral structure and other practical issues are studied. Computer simulations accompanied with experimental results are presented in the paper.

Introduction

Multilevel power conversion has been receiving increasing attention in the past few years for high power applications [1], [2]. Numerous topologies have been introduced and studied extensively for utility and drive applications in the recent literature. These converters are suitable in high voltage and high power applications due to their ability to synthesize waveforms with better harmonic spectrum and attain higher voltages with a limited maximum device rating.

Recent trends in power semiconductor technology indicate a trade-off in the selection of power devices in terms of switching frequency and voltage sustaining capability [3]. Normally, the voltage blocking capability of faster devices such as Insulated Gate Bipolar Transistors (IGBT) and the switching speed of high voltage devices like Integrated Gate Commutated Thyristors (IGCT) [4] is found to be limited. With a modular H-bridge topology [5], realization of multilevel inverters using a hybrid approach involving IGCTs and IGBTs operating in synergism is possible. Hybrid multilevel inverter topologies have been studied for high power applications in [6]–[10]. The topology presented in reference [9] combines a Gate Turn-Off (GTO) thyristor based inverter and an IGBT inverter, similar to that shown in Figure 1. It may be easily verified that with a combination of 2.2 kV and 1.1 kV dc bus voltages in this topology, it is possible to synthesize stepped waveforms with seven voltage levels viz. –3.3 kV, –2.2 kV, –1.1 kV, 0, 1.1 kV, 2.2 kV, 3.3 kV at the phase leg output.

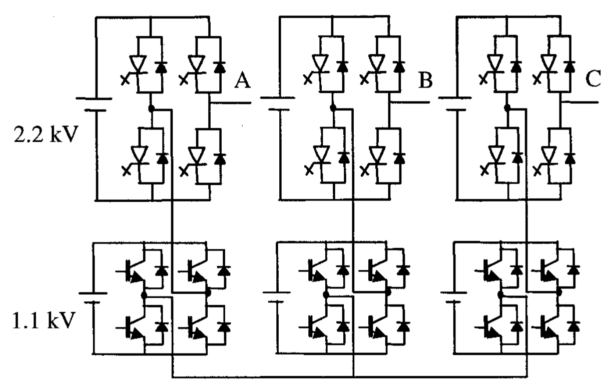

Figure 1. Simplified schematic of the hybrid seven-level inverter.

This paper is devoted to an assessment of various modulation strategies applicable to this inverter. A comparative evaluation of these techniques in terms of attributes such as average switching frequency, dominant harmonics and Total Harmonic Distortion (THD) in the output voltage are reported. The following two sections present the development of high switching frequency techniques, viz. hybrid modulation and the conventional sub-harmonic PWM. This is followed by evaluation of low switching frequency techniques, viz staircase modulation and programmed PWM. The paper concludes with a discussion of advantages and disadvantages of these control strategies.

Hybrid Modulation Technique

The motivation behind investigating the hybrid topology is the pursuit of a synergistic approach, which combines the fast switching ability of IGBTs and large voltage blocking capability of IGCTs. As shown in Figure 1, the higher voltage levels (±2.2 kV) are synthesized using IGCT inverters while the lower voltage levels (±1.1 kV) are synthesized using IGBT inverters. But it is well known that the switching capability of thyristor based devices is limited at higher frequencies [4]. Hence a hybrid modulation strategy which incorporates stepped synthesis in conjunction with variable pulse width of consecutive steps has been presented in [9]. Under this modulation strategy, the IGCT inverter is modulated to switch only at fundamental frequency of the inverter output while the IGBT inverter is used to switch at a higher frequency (f_c). The modulation process and the state of the inverters for various levels of command signals is summarized in Table I.

Table I. Hybrid modulation scheme

Desired Output between	IGCT Inverter	IGBT Inverter
−3.3 and −2.2 kV	−2.2 kV	0 ↔ −1.1 kV
−2.2 and −1.1 kV	−2.2 kV	0 ↔ 1.1 kV
−1.1 and 0.0 kV	0 kV	0 ↔ −1.1 kV
0.0 and 1.1 kV	0 kV	0 ↔ 1.1 kV
1.1 and 2.2 kV	2.2 kV	0 ↔ −1.1 kV
1.1 and 3.3 kV	2.2 kV	0 ↔ 1.1 kV

a ↔ b : Switching between a and b

With this hybrid modulation strategy, the effective spectral response of the output depends on the IGBT switching, while the overall voltage generation is decided by the voltage ratings of the IGCTs. This is illustrated in Figure 2. Figure 3 shows line-line voltage waveform and harmonic spectrum for the same operating point. As expected, the harmonic power is seen to be clustered at the side bands of twice the switching frequency which is 1440 Hz.

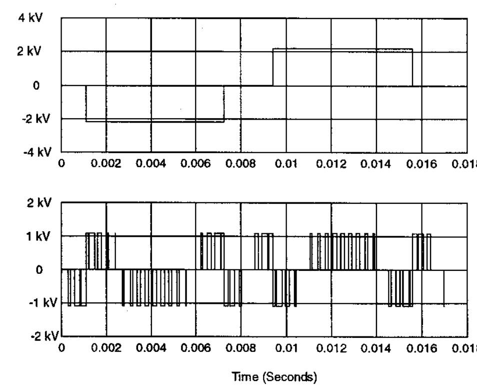

a) IGCT and IGBT inverter voltages.

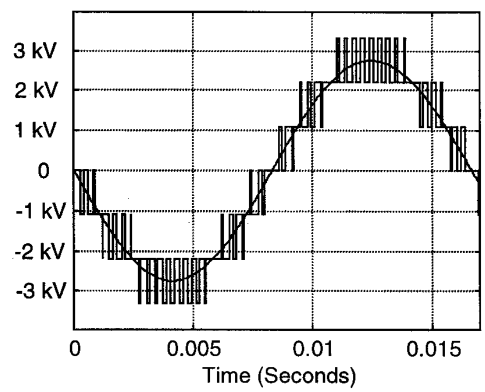

b) Hybrid inverter phase leg voltage.

Figure 2. Representative leg waveforms for hybrid modulation, M = 0.83 and f_c = 1440 Hz.

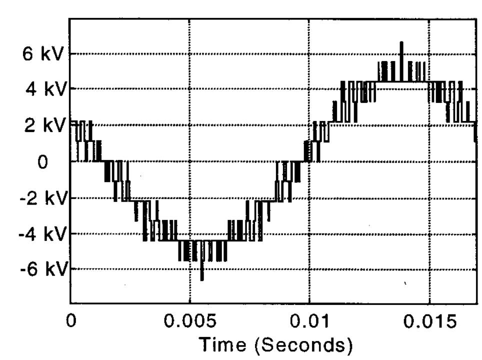

a) Line-line voltage.

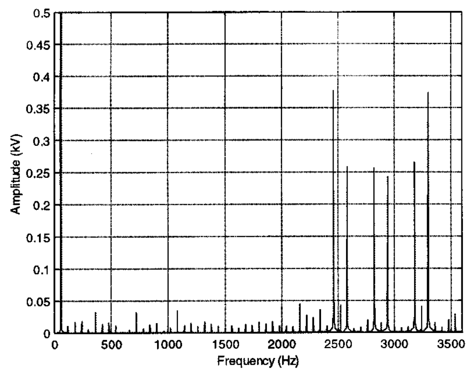

b) Harmonic spectrum of the line-line voltage

Figure 3. Representative line waveforms for hybrid modulation, M = 0.83 and f_c = 1440 Hz.

For spectral analysis, reference command to the hybrid inverter can be represented as

$$V_{ref} = M \cos \omega t \qquad (1)$$

where M is the modulation depth which varies between $0 \leq M \leq 1$ and ω is angular frequency of the reference signal. So the IGCT inverter output and the IGBT inverter leg command are given by

$$V_{IGCT} = \Sigma \frac{8}{3n\pi} \sin \{n\cos^{-1}\frac{1}{3M}\} \cos n\omega t \qquad (2)$$

(for odd n)

$$V_{IGBT\,(command)} = M \cos \omega t \; - \; \Sigma \frac{8}{3n\pi} \sin \{n\cos^{-1}\frac{1}{3M}\} \cos n\omega t \text{ (for odd n)} \qquad (3)$$

Now, spectrum of a naturally sampled sine-triangle PWM single phase Voltage Source Inverter (VSI) with a leg command $A\cos \omega_0 t$ and carrier frequency ω_c is given in [11] as follows

$$V_{VSI} = A\cos \omega_0 t + \frac{4}{\pi} \Sigma \Sigma \frac{1}{2m} J_{2n-1} Am\pi \cos \{2m\, \omega_c t + (2n-1)\, \omega_0 t\} \qquad (4)$$

(summations from m = 1 to ∞ and n = $-\infty$ to $+\infty$)

One can substitute Equation (3) in (4) and obtain a complete spectrum for the PWM IGBT inverter. This when added to the spectrum of the IGCT inverter (Equation (2)) gives a complete spectrum of the hybrid inverter. It may be noted from Equation (4) that there exists a term $A\cos \omega_0 t$ in the spectrum of the VSI output when modulated with a reference $A\cos \omega_0 t$. Hence the low frequency harmonics generated by the IGCT inverter will be cancelled by the corresponding terms in the spectral output of the IGBT inverter, and there will only be side bands at multilples of carrier frequency. This can be verified from the spectrum of the output voltage in Figure 3b.

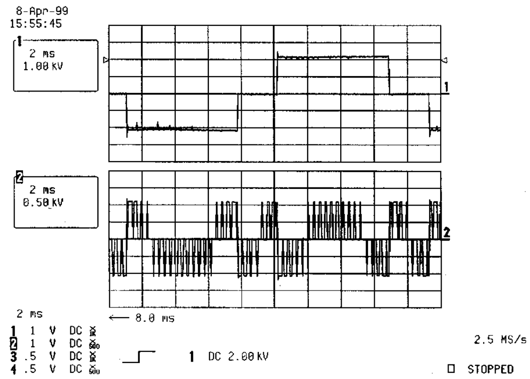

Figure 4. Experimental IGCT and IGBT inverter waveforms, M = 0.83 and f_c = 1440 Hz.
Trace 1. IGCT inverter voltage 1000V/div
Trace 2. IGBT inverter voltage 500V/div

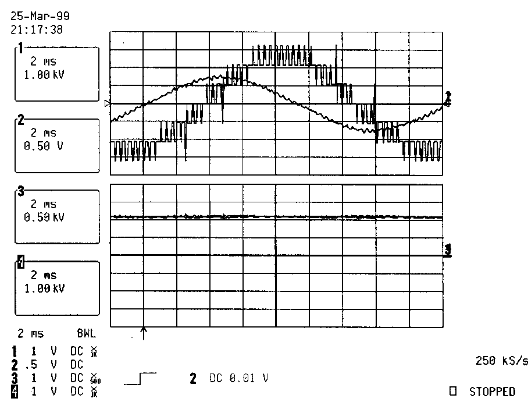

Figure 5. Experimental load and dc bus voltage waveforms, M = 0.83 and f_c = 1440 Hz.
Trace 1. Output voltage 1000V/div
Trace 2. Output current 5A/div
Trace 3. IGBT dc bus 500V/div
Trace 4. IGCT dc bus 1000V/div

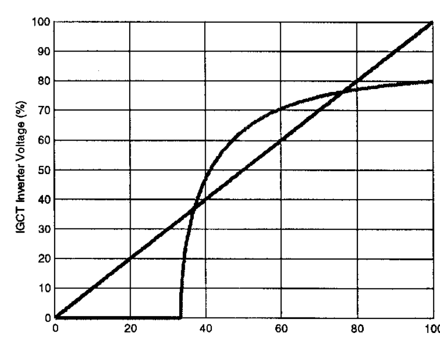

Figure 6. IGCT inverter fundamental voltage.

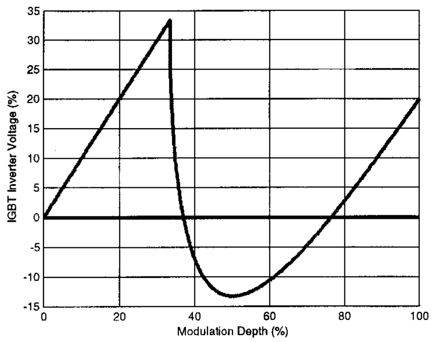

Figure 7. IGBT inverter fundamental voltage.

Particularly, behavior of the individual inverters at fundamental frequency is interesting. The IGCT inverter output under hybrid modulation is plotted against the modulation depth in Figure 6. It is overlaid on a unity slope line which specifies the commanded fundamental voltage. It may be observed that the IGCT inverter synthesizes more voltage than necessary between the modulation depths around 37% and 78%. Hence it is necessary for the IGBT inverter to cancel this excessive voltage and this is illustrated in Figure 7. As may be seen from the fundamental voltage synthesized by the IGBT inverter, this inverter synthesizes negative voltage in this region of modulation depths. In terms of real power flow, which is represented by the current component that is in phase with the fundamental voltage, it appears that the IGCT inverter feeds the power into the IGBT inverter in this zone.

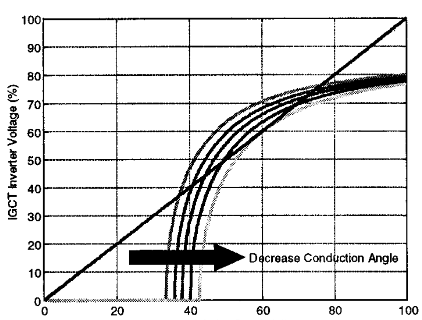

Figure 8. Conduction angle control of the IGCT inverter.

A simple solution for this problem is to control the conduction angle of the IGCT inverter such that the fundamental voltage generated by this inverter is always less than the total commanded voltage. In this mode, the IGBT inverter always adds the voltage and never has to regenerate the power flow. This control scheme is illustrated in Figure 8. In the original hybrid modulation strategy, the IGCT inverter starts contributing as soon as the command reaches 0.33 p.u. As may be observed from Figure 8, this contribution switching time is delayed in terms of modulation depth so as to narrow down the pulse width thereby decreasing the synthesized fundamental voltage. Although this solution does solve the problem of power interaction between the two inverters, it suffers from a higher harmonic distortion than the original hybrid modulation scheme. Simulation and experimental work to verify the feasibility of this approach is under way and will be reported in near future [12]. So also, a more sophisticated version of the solution to solve this problem with a regenerative rectifier is treated in a separate publication [13].

Sub-harmonic Pulse Width Modulation (SPWM) Technique

Conventional SPWM strategies for multilevel inverters employ extensions of carrier-based techniques used for two-level inverters. It has been reported that the spectral performance of a five-level waveform can be significantly improved by employing alternative dispositions and phase shifts in the carrier signals [14], [15]. This paper extends this concept to a seven-level case where the available options for polarity and phase variation increase nearly two-fold. Basically, the SPWM techniques can be broadly categorized into two groups:

Carrier Polarity Variation (Pol. Var.): This method is based on a comparative evaluation of possible dispositions of triangular carrier waveforms depending on their relative polarities. For an m-level inverter this technique requires m-1 carrier signals, which are compared to a reference sine wave. Thus, for a seven-level inverter the number of carrier signals is six and there exists five possible carrier signal configurations. The carriers are named +3V, +2V, +V, –V, –2V and –3V after their dc position. Their phase position is + for a carrier in phase and – for a carrier 180° out of phase. The different configurations are shown in Table II.

Table II: Carrier polarity configurations for a seven-level modulator.

	Carrier Polarity					
	+3V	+2V	+V	-V	-2V	-3V
A	+	+	+	+	+	+
B	+	-	+	-	+	-
C	+	+	+	-	-	-
D	+	-	-	+	+	-
E	+	+	-	+	-	-

This table presents five possible dispositions of triangular carrier waveforms based on their relative polarities. It may be observed that Type A has carriers with the same polarity while in Type B, alternate carriers are flipped. In Type C, all the carriers above zero level have same relative polarity but are in opposition with those below the zero level. Types D and E are additional variations of the carrier signal configurations.

All the different types of polarity variations are simulated in MATLAB Simulink. Simulation studies indicate that the spectral structure of the output with each pattern of carrier disposition is different and a small difference in the respective THD values has been observed. A representative sub-harmonic PWM waveform is shown in Figure 9. It may be seen that the spectral power is spread out around the carrier frequency and the harmonics are clustered at the side bands.

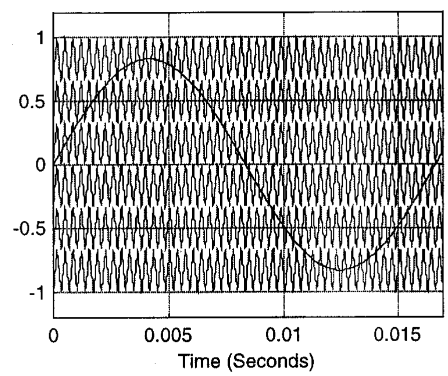

a) Reference and carrier signals.

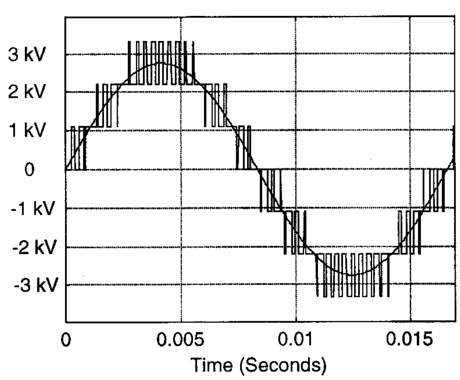

b) Phase leg voltage.

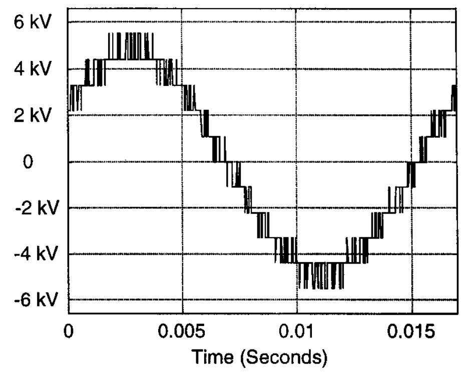

c) Line-line voltage.

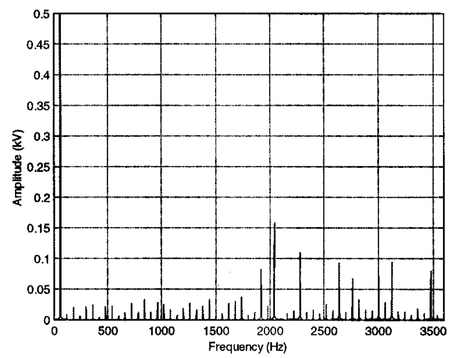

d) Harmonic spectrum of the line-line voltage

Figure 9. Representative waveforms for SPWM with Type A carrier polarity variation, M = 0.83 and f_c = 1440 Hz.

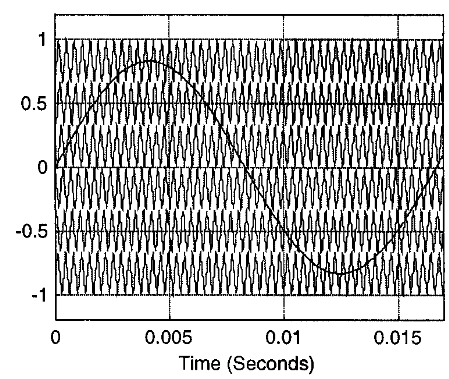

a) Reference and carrier signals.

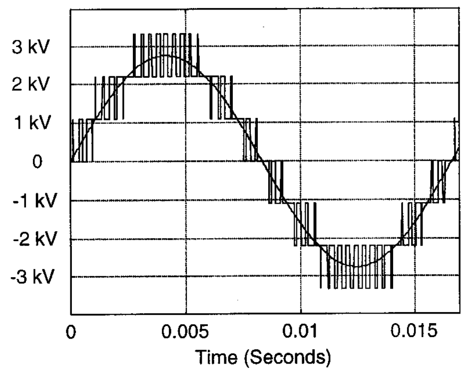

b) Phase leg voltage.

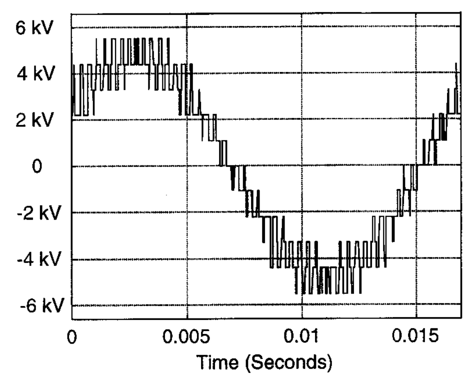

c) Line-line voltage.

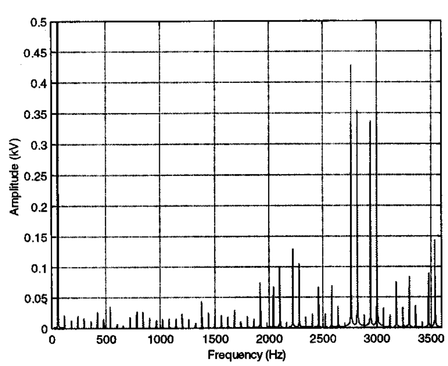

d) Harmonic spectrum of the line-line voltage

Figure 10. Representative waveforms for SPWM with carrier phase variation, $M = 0.83$ and $f_c = 1440$ Hz.

Carrier Phase Variation (Phase Var.): This technique uses a number of carriers that are phase shifted with each other. For a seven-level inverter six carrier signals are phase shifted by 60^o as shown in Figure 10. It may be observed that the spectral structure is different from the carrier polarity variation presented in Figure 9. So also, the output voltage and current THD are poor when compared with other SPWM techniques.

Staircase Modulation Technique

One can synthesize a simple seven-level staircase waveform at the phase leg output with the candidate hybrid topology as shown in Figure 11. As may be observed from Figure 1, the inverters can synthesize 0, ±1.1 kV and ±2.2 kV independently. In addition, levels ±3.3 kV can be obtained by combining ±1.1 kV and ±2.2 kV. Although this strategy is not particularly attractive in terms of spectral quality, it is desirable to operate the inverter in such overmodulation regions for improved dc bus and device utilization. So also, this strategy needs only low switching frequency capability from the devices. However, it is possible to optimize the switching angles of the individual inverters (α_i) for a given modulation index M, so as to minimize a set of dominant harmonics in the output [16].

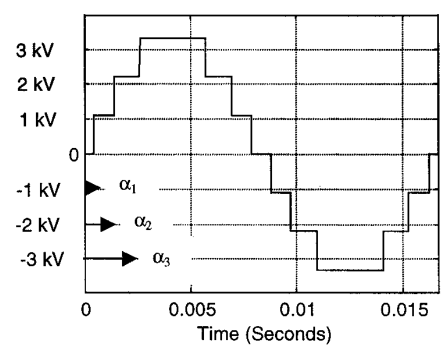

Figure 11. Staircase modulation and definition of switching angles.

To obtain an optimization cost function, the Fourier coefficients of the output voltage can be derived as follows

$$H(n) = V_{dc2} \frac{4}{\pi} \frac{1}{n} [\cos(n\alpha_1) + \cos(n\alpha_2) + \cos(n\alpha_3)] \quad (5)$$

where $V_{dc2} = 1.1$ kV and $n = 1, 3, 5, 7, \ldots$

It may be verified that if all the switching angles are set to zero, the output falls back to a conventional two-level waveform and the fundamental voltage in this case is given by

$$H_{max}(1) = 3\, V_{dc2} \frac{4}{\pi} \quad (6)$$

Since one has three degrees of freedom (three α_i's), one can control three independent parameters simultaneously. It can be calculated that the maximum attainable fundamental voltage with elimination of first three harmonics viz. 5th, 7th and 11th, is 92% of $H_{max}(1)$. For lower values of fundamental voltage, it is required to solve Equations (7)-(9) for switching angles to eliminate the 5th and 7th harmonic components. It may be noted that 5th and 7th are the most dominant harmonics since the even harmonics are cancelled because of the half wave symmetry and triplen harmonics are eliminated in a three-phase three-wire system.

$$H(1) = 3\,V_{dc2}\,M \qquad (7)$$

$$H(5) = 0 \qquad (8)$$

$$H(7) = 0 \qquad (9)$$

where $0 \leq M \leq \frac{4}{\pi}$

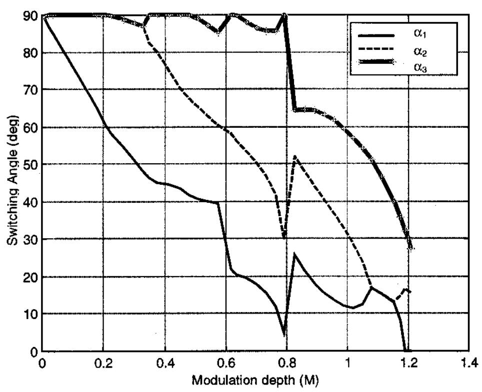

Figure 12. Switching angles for staircase modulation as a function of modulation depth.

To solve equations (7)-(9), a technique as described in [17] can be used. Suppose a vector of angles $\alpha = [\alpha_1, \alpha_2, \ldots, \alpha_n]^T$ satisfies a set of equations $H_i(\alpha) = 0$ to be solved. Then one can formulate an equivalent minimization problem as follows; Let

$$F(\alpha) = \Sigma_{i=1} [H_i(\alpha)]^2 \qquad (10)$$

$F(\alpha)$ is always non-negative, and therefore, if values of α exist for which $F(\alpha) = 0$, these have to be the minimum points for $F(\alpha)$. When $F(\alpha)$ is zero, each $H_i(\alpha)$ must be zero, thus the solution of the set of the equations is to search for the minima of Equation (10). This is done by using MATLAB optimization toolbox and the results from the simulations are given in the graphs presented in Figure 12.

It may be observed that as the modulation depth approaches $4/\pi$, the switching angles approach zero which results in a conventional six-step inverter waveform. So also, as one decreases the modulation depth, the switching angles approach 90° one by one, which means, the phase leg voltage converts from seven-level to five-level and eventually to three-level mode.

A representative staircase modulated waveform is shown in Figure 13. It may be seen that the 5th (300 Hz) and the 7th (420 Hz) harmonics are eliminated from the harmonic spectrum of line-line voltage.

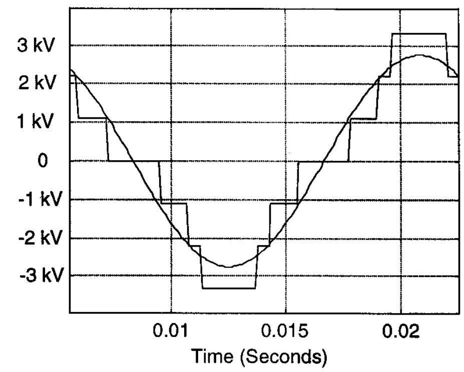

a) Phase leg voltage.

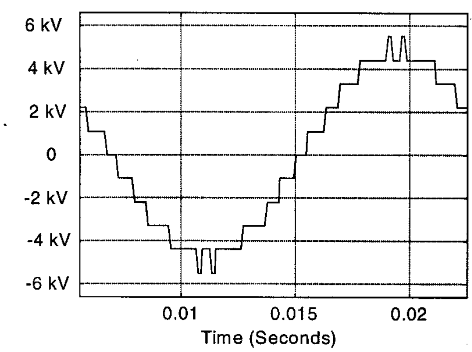

b) Line-line voltage.

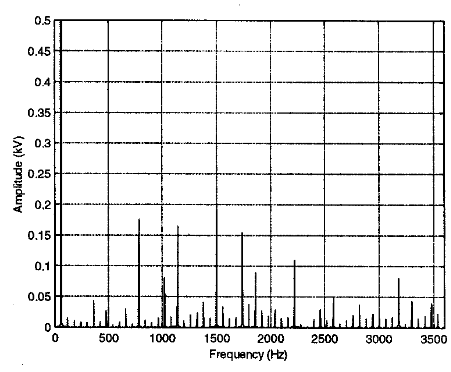

c) Harmonic spectrum of the line-line voltage

Figure 13. Representative waveforms for staircase modulation with optimized switching angles to eliminate 5th and 7th harmonic components, M = 0.83.

Programmed Pulse Width Modulation (PPWM) Technique

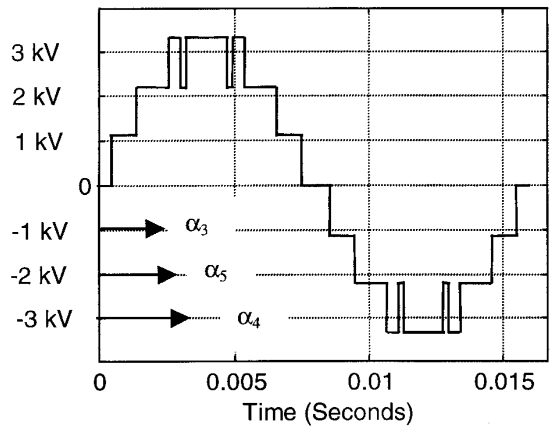

Figure 14. Programmed pulse width modulation and definition of switching angles.

Programmed PWM technique was originally proposed for the conventional two-level inverters [18] and has been extended to multilevel inverters [19], [20]. The basic concept of PPWM is to introduce notches on the staircase and eliminate some more harmonics which are a function of the position and width of the notch. A simplest option is to introduce one notch at the top level as shown in Figure 14. To obtain an optimization cost function, the Fourier coefficients of the output voltage can be derived as follows

$$H(n) = V_{dc2} \frac{4}{\pi} \frac{1}{n} [\cos(n\alpha_1) + \cos(n\alpha_2) + \cos(n\alpha_3) + \cos(n\alpha_4) - \cos(n\alpha_5)] \quad (11)$$

where $V_{dc2} = 1.1$ kV and n = 1, 3, 5, 7, ...

Since one has five degrees of freedom (five α_i's), one can control five independent parameters simultaneously. It is required to solve Equations (12)-(16) for switching angles to eliminate the 5th, 7th, 11th and 13th harmonic components to synthesize the fundamental voltage with a given modulation depth. Although it is possible to introduce more notches in order to cancel more harmonics, it may be noted that the process is computation intensive and the law of diminishing returns sets in quickly with the increasing number of notches. Moreover, it has been observed that elimination of 5th, 7th, 11th and 13th harmonics is sufficient to obtain a satisfactory level of THD in the output current at high power levels.

$$H(1) = 3\, V_{dc2}\, M \quad (12)$$
$$H(5) = 0 \quad (13)$$
$$H(7) = 0 \quad (14)$$
$$H(11) = 0 \quad (15)$$
$$H(13) = 0 \quad (16)$$

where $0 \le M \le \frac{4}{\pi}$

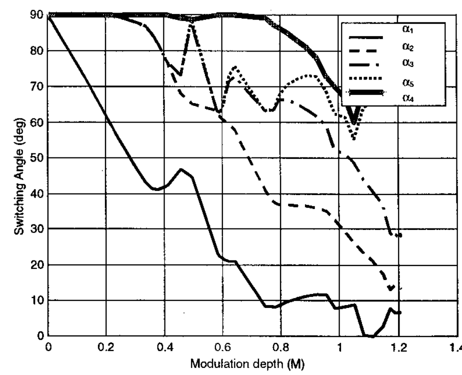

Figure 15. Switching angles for programmed PWM as a function of modulation depth.

The equations are solved by a similar procedure as described in the earlier section and the results are presented in Figure 15. The typical time and frequency domain waveforms are shown in Figure 16. It may be seen that the 5th (300 Hz), 7th (420 Hz), 11th (660 Hz) and 13th (780 Hz) harmonics are eliminated from the harmonic spectrum of line-line voltage.

It may be observed from Figures 12 and 15 that seven-level staircase modulation is suitable in modulation depths from 0.8 to 1.2, whereas PPWM is suitable in region $0.8 \le M \le 1.0$. Simulation results presented so far are done with constant frequency which is a typical case in utility applications. So also, unlike variable frequency drives, such applications normally operate only in a limited range at the higher modulation depths. Hence the simulation results presented so far validate that the hybrid multilevel inverter can be employed for utility applications such as reactive power compensation with programmed PWM in linear and with staircase modulation in overmodulation regions. On the contrary, for drive applications such as constant V/Hz drives, the output fundamental frequency decreases with the output voltage. Hence it is possible to introduce more notches at the lower frequency, thereby eliminating harmonics, however maintaining a constant overall switching frequency. By this reason, one can optimize the PPWM patterns further at lower modulation depths in such cases. But this optimization is application specific and hence not considered in detail here.

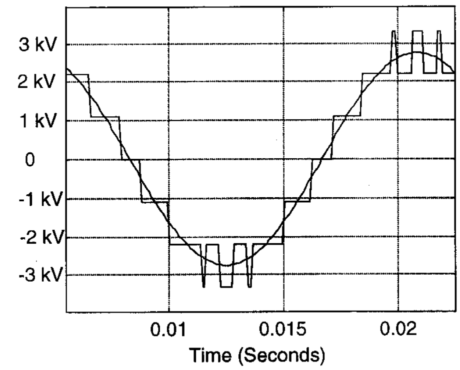

a) Phase leg voltage.

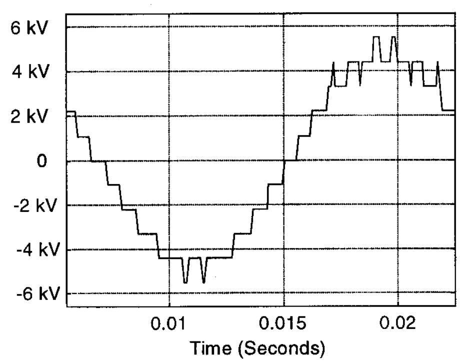

b) Line-line voltage.

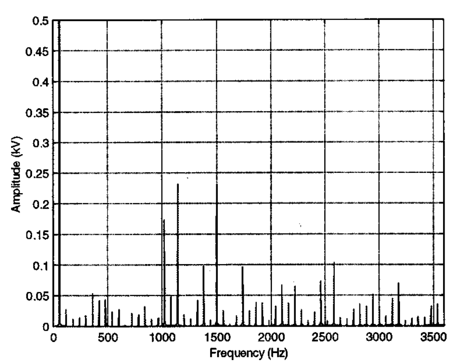

c) Harmonic spectrum of the line-line voltage

Figure 16. Representative waveforms for PPWM with optimized switching angles to eliminate 5^{th}, 7^{th}, 11^{th} and 13th harmonic components, M = 0.83.

Conclusions

This paper has presented a comparative evaluation of various control strategies applicable to the hybrid seven-level inverter. It has been observed that one can obtain superior performance attributes in terms of voltage THD with low frequency techniques such as staircase and PPWM. However, since these strategies optimize the waveforms for a particular set of harmonics, the dominant harmonics are still at low frequencies. On the contrary, the dominant harmonics present in the high frequency techniques are at the side bands of multiples of the switching frequency, but the voltage THD in these cases is relatively poor. A comparison of these techniques is tabulated in Table III.

Table III. Comparison of control strategies.

Modulation Technique	$V_{line-line}$ THD (%)	Dominant Harmonic (Hz)
Hybrid	12.9998	2460 (41^{st})
Pol. Var. SPWM	8.5260	2040 (34^{th})
Phase Var. SPWM	14.6078	2760 (46^{th})
Staircase	6.3573	780 (13^{th})
PPWM	7.1880	1020 (17^{th})

To conclude, it is contended that, in comparison with all the rest of control strategies, application-specific programmed PWM techniques offer excellent THD figures. So also with sufficient number of harmonic elimination notches, the dominant harmonic component can be pushed in high frequency region. Thus, it is possible to obtain a satisfactory spectral performance with relatively low switching frequency.

References

[1] J.S. Lai and F.Z. Peng, "Multilevel Converters - A New Breed of Power Converters," *IEEE-IAS'95 Conference Proceedings*, pp. 2348-2356, 1995.

[2] B.S. Suh, G. Sinha, M.D. Manjrekar, T.A. Lipo, "Multilevel Power Conversion – An Overview of Topologies and Modulation Strategies", *OPTIM'98 Conference Proceedings*, pp. AD-11-AD-24, 1998.

[3] B.J. Baliga, *Power Semiconductor Devices*, PWS Publishing Company, 1996.

[4] P.K. Steimer, H.E. Gruning, J. Wuninger, E. Caroll, S. Klaka, S. Linder, "IGCT – A New Emerging Technology for High Power, Low Cost Inverters," *IEEE-IAS'98 Conference Proceedings*, pp.1592-1599 ,1998.

[5] M. Marchesoni, M. Mazzucchelli, S. Tenconi, "A Non Conventional Power Converter for Plasma Stabilization," *IEEE-PESC'88 Conference Record*, pp. 122-129, 1988.

[6] H. Gruning, "Power Electronic Circuit Arrangement having Plural Power Converters," U.S. Patent No. 5,805,437, 1998.

[7] S.H. Hosseini and R.M. Mathur, "A Binary Multilevel Voltage Source Inverter for Static VAr Generation," *IEEE-CCECE'97 Conference Proceedings*, pp. 427-430, 1997.

[8] A. Damiano, M. Fracchia, M. Marchesoni, I. Marongiu, "A New Approach in Multilevel Power Conversion," *EPE'97 Conference Record*, pp. 4.216-4.221, 1997.

[9] M.D. Manjrekar and T.A. Lipo, "A Hybrid Multilevel Inverter Topology for Drive Applications," *IEEE-APEC'98 Conference Proceedings*, pp. 523-529, 1998.

[10] M.D. Manjrekar and T.A. Lipo, "A Generalized Structure of Multilevel Power Converter," *IEEE-PEDES'98 Conference Proceedings*, 1998.

[11] D.M. Divan and T.A. Lipo, *Class Notes for ECE 712 - Solid State Power Conversion Course*, University of Wisconsin – Madison, Fall 1995.

[12] M.D. Manjrekar, *Topologies, Analysis, Controls and Generalization in H-Bridge Multilevel Power Conversion*, Ph.D. Thesis, University of Wisconsin-Madison, In preparation.

[13] M.D. Manjrekar, R. Lund, P. Steimer, T.A. Lipo, "Hybrid Multilevel Power Conversion System – A Competitive Solution for High Power Applications," To be presented at *IEEE-IAS'99 Annual Meeting*, 1999.

[14] G. Carrara, S. Gardelta, M. Marchesoni, "A New Multilevel PWM Method: A Theoretical Analysis," *IEEE Trans. on Power Electronics,* Vol. 7, No. 3, July, pp. 497-505, 1992.

[15] V. Agelidis, M. Calais, "Application Specific Harmonic Performance Evaluation of Multicarrrier PWM Techniques," *IEEE-PESC'98 Conference Record*, pp. 172-178, 1998.

[16] Q. Jiang and T.A. Lipo, "Switching Angles and DC Link Voltages Optimization for Multilevel Cascade Inverters," *IEEE-PEDES'98 Conference Proceedings*, pp. 56-61, 1998.

[17] D.A. Pierre, *Optimization Theory with Applications*, Dover, 1986.

[18] H.S. Patel and R.G. Hoft, "Generalized Techniques of Harmonic Elimination and Voltage Control in Thyristor Inverters: Part I – Harmonic Elimination," *IEEE Transactions on I.A.*, Vol. IA-9, No. 3, May/June, pp. 310-317, 1973.

[19] P.N. Enjeti and Ranjit Jakkli, "Optimal Power Control Strategies for Neutral Point Clamped Inverter Topology," *IEEE Transactions on I.A.*, Vol. IA-28, No. 3, May/June, pp. 558-566, 1992.

[20] L. Li, D. Czarkowski, Y. Liu, P. Pillay, "Multilevel Selective Harmonic Elimination PWM Technique in Series Connected Voltage Inverters," *IEEE-IAS'98 Conference Proceedings*, pp. 1454-1461, 1998.